Sustainable Chemistry and Pharmacy 31 (2023) 100896

Contents lists available at ScienceDirect

Sustainable Chemistry and Pharmacy

journal homepage: www.elsevier.com/locate/scp

Mechanical and durability performance of alkali-activated slag cement concretes with carbonate and silicate activators

M. Mavroulidou *, I. Sanam, L. Mengasini

Division of Civil and Building Services Engineering, London South Bank University, 103 Borough Road, London, SE1 0AA, UK

ARTICLE INFO

Keywords:
Alkali activated cements
Sodium carbonate and sodium silicate
Ground granulated blastfurnace slag
Sustainable concrete

ABSTRACT

In the race for decarbonization, the construction industry is increasingly turning its interest to alkali-activated cements (AAC) as an alternative to Portland cement (PC). This paper studies sodium carbonate (Na_2CO_3) as a potentially environmentally-friendlier and cheaper activator of ground granulated blastfurnace slag (GGBS) in comparison to Na_2SiO_3 or combined Na_2SiO_3-Na_2CO_3 activators. The laboratory study started with an investigation of suitable mixing procedures, after which mechanical and durability testing was performed under four curing conditions. Ambient temperature with high-moisture curing gave better strength gain in time, whereas thermal curing gave the highest early strengths and lowest absorption and porosities but strengths stopped evolving at later times. The strengths of all tested AAC mixes were suitable for structural concrete although those containing Na_2SiO_3 had the highest strengths at all curing conditions and ages. For the mix with Na_2CO_3 only (suitable for C30/40 grade concrete vs C50/60 concrete for the mixes containing Na_2SiO_3) strengths were evolving considerably with curing time despite the lower early strengths. All mixes with AAC performed better in terms of chloride attack (accelerated corrosion test) compared to the PC mix, despite their higher water absorption and, in most cases, porosity. AAC mixes with Na_2CO_3 only (as activator) were the least affected in terms of strength after exposure to sulphates. Overall, the study gives promise that Na_2CO_3-activated slag can be a good AAC system as alternative to PC towards an increased sustainability in the construction sector.

1. Introduction

Concrete containing Portland cement (PC) is the most widely used building material and is integral to modern life. However, the production of PC which is reported to be 4 billion tonnes of CO_2 per annum, generates 8% of global man-made greenhouse gas emissions (Ellis et al., 2020). There is thus an urgent need for alternative cements that would lower the environmental footprint of concrete production, without incurring high costs for their manufacture. Alkali-Activated cements (AAC), i.e., PC-free binders originating from the reaction of an alkali metal source with an (alumino-) silicate, have thus been increasingly attracting attention worldwide as alternatives to PC (Mavroulidou et al., 2021). This is because AAC are claimed to have an overall lower environmental footprint than PC. This is linked to their lower energy demand and CO_2 emissions for their production and the added advantage of providing recycling routes for a number of waste materials or industrial by-products which can be used in the AAC composition thus further increasing the environmental benefits of using these cements. Examples of by-products or waste materials rich in silica and alumina proposed as precursors in AAC include ground granulated blastfurnace slag (GGBS), fly ash (FA), waste glass, waste quarry materials or

* Corresponding author. Division of Civil and Building Services Engineering, London South Bank University, 103 Borough Road, London, SE1 0AA, UK.
E-mail address: mavroum@lsbu.ac.uk (M. Mavroulidou).

https://doi.org/10.1016/j.scp.2022.100896
Received 27 April 2022; Received in revised form 29 October 2022; Accepted 2 November 2022
Available online 25 November 2022

construction spoil -e.g., containing waste clays- or incinerated municipal solid waste (Luukkonen et al., 2018). In the past, such materials i.e., combustion ashes as well as slags (e.g., steel slags) were stockpiled entailing environmental risks, as they may contain elevated heavy metal contaminants. Landfilling them also entails costs (see e.g., landfill taxes), and environmental and aesthetics issues, and becomes unsustainable due to the limited available space for landfills. Considering the production of over 25 billion tonnes of concrete per annum (Imbabi et al., 2012), the commercial use of AAC can greatly reduce the need of landfilling, whilst also encapsulating/incorporating potentially hazardous materials in the cement. Considerable estimated overall sustainability improvements of AAC compared to PC were reported in the literature. Namely, Davidovits (2013) mentioned potentially a 5–6 times reduction in the environmental footprint of geopolymer AAC whereas up to 55%–75% less CO_2 emissions than PC from the cradle to pre-construction were estimated in Yang et al. (2013) for alkali activated Ground Granulated Blastfurnace Slag (GGBS). A number of other recent papers also corroborate the environmental advantages of using AAC in terms of global warming potential or embodied energy (Salas et al., 2018; Jamieson et al., 2015; Passuello et al., 2017). Literature also shows that AAC can perform better than PC in terms of physical and chemical deterioration of concrete (Palomo et al., 2014; Ma et al., 2016; Krivenko, 2017; Ke et al., 2017 (a),(b); Criado and Provis, 2018; Mengasini et al., 2021; Krivenko et al., 2021 amongst many other).

Based on the above, AAC play a major role in green chemistry for cement production due to their ability in incorporating a wide range of value-added wastes, for improved resource efficiency as well as better accessibility of AAC to developing communities, their potential for lower energy and emissions linked to cement production thus less harm to the environment and the reported improved performance and durability of alkali-activated cements compared to Portland cement.

Despite these advantages, the most widely studied activators to-date, i.e. sodium silicate (Na_2SiO_3), sodium hydroxide (NaOH) or their combination, are expensive and have high energy input requirements for their production, unless they are derived from some waste material (see e.g., Tchakouté et al., 2016 or Passuello et al., 2017 mentioned above); they also suffer from rapid hardening, (resulting in concrete difficult to cast), and a high causticity, causing health and safety concerns during their handling.

To address these issues, this paper studies instead sodium carbonate (Na_2CO_3) as a potentially cheaper and environmentally-friendlier suitable alternative activator. As Bernal et al. (2016) note, Na_2CO_3 can result from industrial processes (as a secondary product), or otherwise by alkali-carbonate deposit mining, subject to thermal treatment at moderate temperatures, and is less caustic, due to its lower pH compared to hydroxides. Carbonates (e.g. Na_2CO_3) or carbonate/hydroxide mixtures were used as activators of industrial slags in the former Soviet Union (mostly Ukraine) to produce concretes. These demonstrated a very good durability under harsh environments and conditions that PC would not have been able to withstand; they also showed strength gains over their service life (Xu et al., 2008). Yet, there is a very limited international literature in English on these AAC systems (see e.g., Li and Sun 2000; Fernández-Jiménez and Puertas, 2003; Bernal et al., 2015, 2016; Kovtun et al., 2015; Abdalqader et al., 2016 or hybrid OPC-AAC systems by Garcia-Lodeiro et al., 2015) which is also pointed out in RILEM report (2014); the available literature focuses mostly on the detailed characterisation of the resulting cements (see e.g., Bernal et al., 2015 or 2016) or the compressive strength of cements and mortar mixes rather than properties and durability of concrete with Na_2CO_3 AAC.

To fill this knowledge gap, the presented paper focuses on properties of concrete incorporating Na_2CO_3 AAC cements unlike the existing studies. As there is very limited literature on the topic, this is a considerable contribution to knowledge. A number of identified novelties of the paper are:

a) the study of the effect of mixing procedure/sequence as well as curing conditions on these little researched systems, as literature on other AAC systems indicated that the results could be highly dependent on these (see e.g., Bakharev et al., 1999; RILEM, 2014; Mavroulidou and Shah, 2021; Parathi et al., 2021; Nodehi et al., 2022). To the Authors' knowledge there is no previous study on the effect of mixing sequence and procedure on this type of AAC; even for other AAC systems in general there are hardly any studies on the effect of the mixing procedure with few exceptions for cement or mortar (not concrete) including Palacios and Puertas (2011) who studied the effect of mixing time for slag paste and mortars -not concrete- activated by waterglass, and recently the study of the effect of mixing time and procedure on alkali-activated slag-silica fume cement pastes -but not concrete- (Kim & Kang, 2020). The effect of different curing methods for these AAC systems was also not researched to the Authors' knowledge.
b) Furthermore, the paper presents comparative results of a wide range of mechanical and also durability tests on concrete with Na_2CO_3 which are lacking in the literature.
c) Similarly, a comparison of the mechanical and durability performance of Na_2CO_3-Na_2SiO_3 AAC, and Na_2SiO_3 AAC concretes, is lacking in the literature.

2. Materials and experimental procedures

2.1. Materials and concrete mixes

The precursor was commercially-supplied GGBS whose suitability for AAC based on a number of characteristics (e.g., vitreous content ≥90%), specific surface between 490 and 540 m^2/kg, and pH > 10) was discussed in Mavroulidou and Martynková (2018). CEMI 52.5 N (regular cement) was also used so that the performance of AAC concrete can be compared against regular concrete with PC. The results for this CEM-I were published in Mengasini et al. (2021). The chemical composition of CEM-I and GGBS is shown in Table 1. Activators were commercially supplied analytical grade sodium silicate Na_2SiO_3 solution of a molarity of ca. 3.2 M and anhydrous sodium carbonate Na_2CO_3 pellets (of purity ≥99%). For tests where Na_2CO_3 was supplied in solution the molarity varied between approximately 1.4 M to approximately 2.1 M (in the former case Na_2CO_3 was dissolved in all concrete water, whereas in the latter only part of the total water was supplied, sufficient to dissolve the Na_2CO_3 pellets at room temperature). The particle size distri-

Table 1
Typical oxide composition of GGBS and CEM-I according to suppliers' information (reported as oxide wt.%).

Oxide composition	GGBS (%)	CEM-I (%)
CaO	40	63.48
SiO_2	36	20.62
Al_2O_3	12.5	4.81
MgO	7.74	1.07
Fe_2O_3	0.5	2.71
Na_2O		0.21
K_2O		0.52
SO_3	0.1	3.10
P_2O_5		
TiO_2	0.9	
MnO	0.5	
Other		

bution (PSD) of the dry concrete mix components (coarse aggregates (gravel), fine aggregate (river sand), cement and GGBS) is shown in Fig. 1.

Table 2 shows the concrete mix design. A liquid-to-solid ratio (l/s) of 0.55 was kept for all mixes to ensure consistency of comparisons.

2.2. Curing procedures

For each mix four different curing methods were studied, according to processes used by different researchers testing AAC (see also Mavroulidou and Martynková, 2018; Mavroulidou and Shah, 2021): (a) Method 1 (water-curing): curing at room temperature inside the moulds for 72h (or up to 96h if specimens were still too soft at 72h to demould, as for mix 1 - consistently with Fernández-

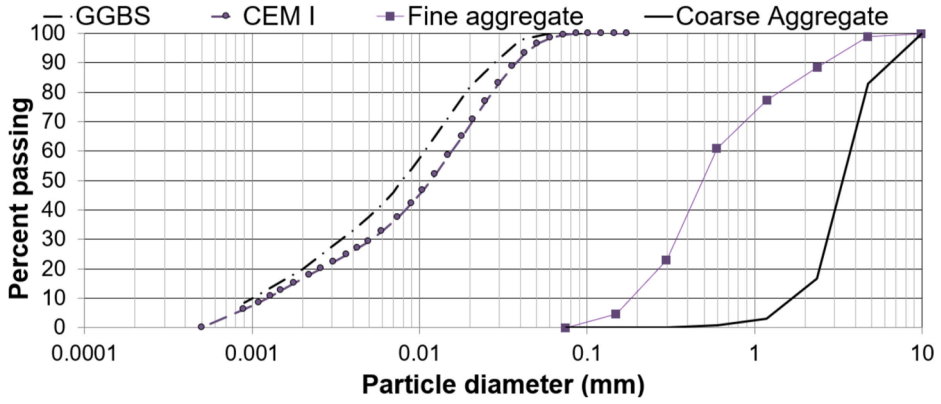

Fig. 1. PSD of coarse and fine aggregate, GGBS and CEM I.

Table 2
Mix design (kg).

Mix #	CEM I	GGBS	Fine aggregate (Sand)	Coarse aggregate	Na_2CO_3 Powder	Na_2SiO_3	Additional Water[a]	l/s ratio[b]
Mix1(a) (Na_2CO_3 powder)	0	415	784	1039	37	0	249	0.55
Mix1(b) (Na_2CO_3 solution)	0	415	784	1039	37	0	81	0.55
Mix2(a) (Na_2CO_3 powder + Na_2SiO_3 solution)	0	415	784	1039	18.5	46.25	221.25	0.55
Mix2(b) (Na_2CO_3 solution + Na_2SiO_3 solution)	0	415	784	1039	18.5	46.25	137.25	0.55
Mix 3 Na_2SiO_3 solution	0	415	784	1039	0	92.5	193.5	0.55
Control mix: CEM-I[c]	415	0	784	1039	0	0	230	0.55

[a] In addition to that in solutions.
[b] l/s is the liquid-to-solid ratio, which includes solids/water in activator solutions.
[c] Tests with this mix were previously performed by Mengasini (see Mengasini et al., 2021).

Jiménez and Puertas, 2003 or Bernal et al., 2016), followed by water-curing at 20ºC, until required for testing; (b) Method 2 (ambient-temperature sealed curing): constant moisture curing, with samples kept in moulds, covered by an impermeable membrane to preserve their original moisture content; (c) Method 3 (thermal curing): curing at 65 °C for 5.5 h, then, after overnight cooling, demoulding and water-curing at 20ºC; (d) Method 4: (high-humidity curing) in a temperature and humidity-controlled cabinet, at a relative humidity of 95% and a temperature of 25 °C.

2.3. Testing procedures

The mechanical properties of hardened concrete mixes which were tested included (a) the cube compressive strength at different curing times of triplicate 100 mm cubes following BS EN 12390–3:2019 (BSI, 2019a) and (b) the tensile strength of concrete performing splitting cylinder strength tests of duplicate 300 mm in height and 150 mm in diameter cylinders tested following BS EN 12390–6:2019 (BSI, 2019b). For both compressive and splitting cylinder testing a 2000 kN compression testing plant was used.

The durability of concrete specimens was assessed based on: (a) water absorption (immersion and capillary rise); (b) effective porosity; (c) accelerated corrosion testing (to assess resistance to chloride attack) and (d) sulphate attack resistance. A brief description of the tests and their relevance follows below:

2.3.1. Water absorption

Duplicate 70 mm cube specimens, were used for water absorption testing (by capillary rise and immersion) according to BS1881–122:2011 (BSI, 2011), which offers an indication of the ease of deleterious ion transportation (through water) into the concrete. Cured specimens for 28 and 56 days respectively were oven-dried at 105 °C for 72 ± 2 h, weighed and left to cool in air-tight container for 24 ± 0.5 h, then tested by immersion in water for 30 min; calculation of the water was based on the % ratio of the increase in the cube mass after 30 min of immersion, over the dry cube mass. For capillary absorption sealed specimens (with insulation tape) were left to absorb water from the base of the specimen while measurements of mass and water rise in the sample were made at regular intervals up to at least 4 h of exposure to water.

2.3.2. Effective porosity

Linked to transport properties of concrete is also its effective porosity; this was determined from duplicate cylindrical specimens (70 mm in height and 38 mm in diameter) oven-dried at 105 °C for 72 ± 2h, and left to cool for 24 h in an air-pump vacuum vessel), using a helium porosimeter apparatus.

2.3.3. Resistance to chloride attack

Embedded steel reinforcement corrosion due to chloride attack causes concrete to deteriorate, (cracking and spalling of concrete). Accelerated corrosion tests were performed to assess embedded rebar corrosion. Impressed current density testing was performed on duplicate 100 mm cube specimens using the methodology and apparatus described in Mavroulidou (2017) and Mengasini et al. (2021), namely: (a) 100 mm cubes with an embedded pre-weighed carbon steel rebar (8 mm diameter), at the centre of the cubes; (b) equipment consisting of a data logger, a 10V DC power supply, 2 stainless-steel plates and a plastic bucket containing 3.5% of NaCl solution. Due to practical limitations in the amount of specimens that could be tested in the laboratory for corrosion, indicatively only one method of curing was used, i.e. method 4. After curing in the humidity cabinet for 7 days, the specimens were immersed into the NaCl solution and subjected to accelerated corrosion testing for 21 days, after which the steel rebars were removed from the concrete and cleaned following ASTM G1-90 (ASTM 2000). The cleaned rebars were weighed and the percentage of steel mass loss due to corrosion calculated. To calculate the corrosion rate Equation (1) was used:

$$Corrosion\ rate = K \cdot \Delta W / (A \cdot T \cdot D) \quad (1)$$

where K = 87.6 (constant); ΔW: rebar mass loss (mg); A: exposed rebar surface area (cm^2); T: time (h); D: density of rebar (i.e. 7.8 g/cm^3).

2.3.4. Resistance to sulphate attack

Sulphates entering the hydrated cement matrix can cause calcium monosulfoaluminates to revert to calcium trisulfoaluminate (ettringite), which leads to expansion and consequently damage of concrete. To assess AAC mix performance against sulphate attack, triplicate 100 mm cube samples cured for 7 days, were immersed in a 50 g/L Na_2SO_4 solution. The length change of the specimens was monitored at three different locations of the specimen using Vernier callipers; measurements were taken at 0, 20, 40, 60, and 90 days. After spending 90 days in the sulphate solution, the specimens were removed and their compressive strength assessed to detect any reductions due to sulphates.

2.4. Preliminary testing

The investigation started with casting and testing duplicate cubes using indicatively curing method 4, to observe comparatively the effect of mixing sequence/procedure on setting behaviour, workability, and 7-day cube compressive strength of the three AAC mixes. The mixing considered (a) supplying Na_2CO_3 as a powder versus in solution; (b) trying a number of combinations in the sequence of mixing the different ingredients, i.e., aggregates, precursor, water and activators (see Table 3). An extended length of mixing time was also used, as recommended in RILEM (2014) for AAC and experienced as beneficial in previous studies of the LSBU group (Mavroulidou and Shah, 2021). Based on the first set of tests, the best overall mixing procedure of those tried was then followed for the complete set of tests of the mixes with Na_2CO_3 only, $Na_2CO_3 + Na_2SiO_3$, and Na_2SiO_3 respectively.

Table 3
Investigations on mixing sequence/procedure.

Mix/ procedure ID	Mixing sequence and time
1a, mixing 1	Mix the GGBS&Na_2CO_3 powders for 2 min; mix the two aggregates for 2 min; Add the GGBS&Na_2CO_3 powder mix to the aggregates and mix for 5 min; Add gradually all water to all the dry ingredients and mix for 5 min; Stop mixing for 3 min; Resume mixing for 5–10 min
1a, mixing 2	Mix the GGBS&Na_2CO_3 powders for 2 min; mix the two aggregates for 2 min; Use some water on the aggregates and mix for 2 min; Add the GGBS&Na_2CO_3 powder then the rest of the water to all ingredients and mix for 5 min; Stop mixing for 3 min; Resume mixing for 5–10 min
1b, mixing 1	Mix the two aggregates for 2 min; Mix the Na_2CO_3 in the required water (considering the solubility of Na_2CO_3 of 220 g/L at 20°C) for 5 min or until dissolved; Add rest of the water to the dry ingredients and mix for 5 min; Add the GGBS in the Na_2CO_3 solution and mix for 5 min; Add the binder solution to the aggregates and mix for 5 min; Stop mixing for 3 min; Resume mixing for 5–10 min
1b, mixing 2	Mix the two aggregates for 2 min; Mix the Na_2CO_3 in all water for 5 min or until dissolved; Add a small part of the activator solution to the dry ingredients and mix for 5 min; Add the GGBS in the mixer and mix for 5 min; Add gradually the rest of the activator solution mix for 5 min; Stop mixing for 3 min; Resume mixing for 5–10 min
1b, mixing 3	Mix the two aggregates for 2 min; Add the GGBS in the aggregate mix and mix for 2 min; Mix the Na_2CO_3 in the required water (considering the solubility of Na_2CO_3 of 220 g/L at 20°C) for 5 min; Add rest of the water to the dry ingredients and mix for 5 min; Add the activator solution to the aggregates & GGBS and mix for 5 min; Stop mixing for 3 min; Resume mixing for 5–10 min
1b, mixing 4	Mix the two aggregates for 2 min; Mix the Na_2CO_3 in all water mix for 5 min or until dissolved; Add the GGBS in the Na_2CO_3 solution and mix for 5 min; Add the binder solution to the aggregates and mix for 5 min; Stop mixing for 3 min; Resume mixing for 5–10 min
2a, mixing 1	Mix the GGBS&Na_2CO_3 powders for 2 min; mix the two aggregates for 2 min; Add the GGBS&Na_2CO_3 powder mix to the aggregates and mix for 3 min; Add gradually all water to all the dry ingredients and mix for 3 min; Add the Na_2SiO_3 solution and mix for 3 min; Stop mixing for 3 min; Resume mixing for 5–10 min
2a, mixing 2	Mix the GGBS&Na_2CO_3 powders for 2 min; mix the two aggregates for 2 min; Add the GGBS&Na_2CO_3 powder mix to the aggregates and mix for 3 min; Add the Na_2SiO_3 solution and mix for 3 min; Add gradually all water to all the dry ingredients and mix for 3 min; Stop mixing for 3 min; Resume mixing for 5–10 min
2b, mixing 1	Mix the two aggregates for 2 min; Add the GGBS powder and mix for 2 min; Mix the Na_2CO_3 in all water for 5 min or until dissolved; Add the silicate solution to the Na_2CO_3 solution; Add gradually the activator solution mix for 5 min; Stop mixing for 3 min; Resume mixing for 5–10 min
2b, mixing 2	Mix the two aggregates for 2 min; Mix the Na_2CO_3 in all water for 5 min or until dissolved; Add the silicate solution to the Na_2CO_3 solution; Add some small part of the activator solution to the dry ingredients and mix for 5 min; Add the GGBS in the mixer and mix for 5 min; Add gradually the rest of the activator solution mix for 5 min; Stop mixing for 3 min; Resume mixing for 5–10 min
2b, mixing 3	Mix the two aggregates for 2 min; Add the GGBS powder and mix for 2 min; Mix the Na_2CO_3 in all water for 5 min or until dissolved; Add gradually the silicate solution to the dry aggregate & GGBS mix; Add gradually the Na_2CO_3 solution and mix for 5 min; Stop mixing for 3 min; Resume mixing for 5–10 min
2b, mixing 4	Mix the two aggregates for 2 min; Mix the Na_2CO_3 in all water; mix for 5 min or until dissolved; Mix the Na_2SiO_3 with the GGBS powder for 3 min; Add the Na_2CO_3 solution and mix for 3 min; Add the binder solution to the aggregates and mix for 5 min; Stop mixing for 5 min; Resume mixing for 5–10 min
2b, mixing 5	Mix the two aggregates for 2 min; Mix the Na_2CO_3 in all water mix for 5 min or until dissolved; Add the silicate solution to the Na_2CO_3 solution; Add the GGBS in the Na_2CO_3&Na_2SiO_3 solution and mix for 5 min; Add the binder solution to the aggregates and mix for 5 min; Stop mixing for 3 min; Resume mixing for 5–10 min
3, mixing 1	Mix the two aggregates for 2 min followed by GGBS and mix for 2 min; Add gradually all water to all the dry ingredients and mix for 3 min; Add the Na_2SiO_3 solution and mix for 5 min; Stop mixing for 3 min; Resume mixing for 5–10 min
3, mixing 2	Mix the two aggregates for 2 min followed by GGBS and mix for 2 min; Add the Na_2SiO_3 solution and mix for 3 min; Add gradually all water and mix for 5 min; Stop mixing for 3 min; Resume mixing for 5–10 min
3, mixing 3	Mix the two aggregates for 2 min followed by GGBS and mix for 2 min; Mix the Na_2SiO_3 solution in all water for 5 min; Add gradually the activator solution mix for 5 min; Stop mixing for 3 min; Resume mixing for 5–10 min
3, mixing 4	Mix the two aggregates for 2 min; Mix the Na_2SiO_3 solution in all water for 5 min; Add some small part of the activator + water solution to the dry ingredients and mix for 5 min; Add the GGBS in the mixer and mix for 5 min; Add gradually the rest of the activator solution for 5 min; Stop mixing for 3 min; Resume mixing for 5–10 min
3, mixing 5	Mix the two aggregates for 2 min followed by GGBS and mix for 2 min; Mix the Na_2SiO_3 solution in half of the water for 5 min; Add gradually the silicate solution to the dry aggregate &GGBS mix and mix for 5 min; Add the rest of the water to the bowl and mix for 5 min; Stop mixing for 3 min; Resume mixing for 5–10 min
3, mixing 6	Mix the two aggregates for 2 min; Mix the Na_2SiO_3 solution with the GGBS powder for 3 min; Add half of the water to the Na_2SiO_3&GGBS mix and mix for 3 min; Add the binder solution to the aggregates and mix for 5 min; Add the rest of the water and mix for 5 min; Stop mixing for 3 min; Resume mixing for 5–10 min
3, mixing 7	Mix the two aggregates for 2 min; Add all water to Na_2SiO_3 solution and mix for 3 min; Add the GGBS into the Na_2SiO_3 solution and mix for 3 min; Add the binder solution to the aggregates and mix for 5 min; Stop mixing for 3 min; Resume mixing for 5–10 min

3. Results and discussion

3.1. Preliminary testing

Fig. 2(a)–(c) shows the 7-day strengths of the three mixes, according to the different mixing sequences and procedures tried (see Table 3). For mix 1, considering the variability of concrete batches, the strength differences are too small in most cases to be

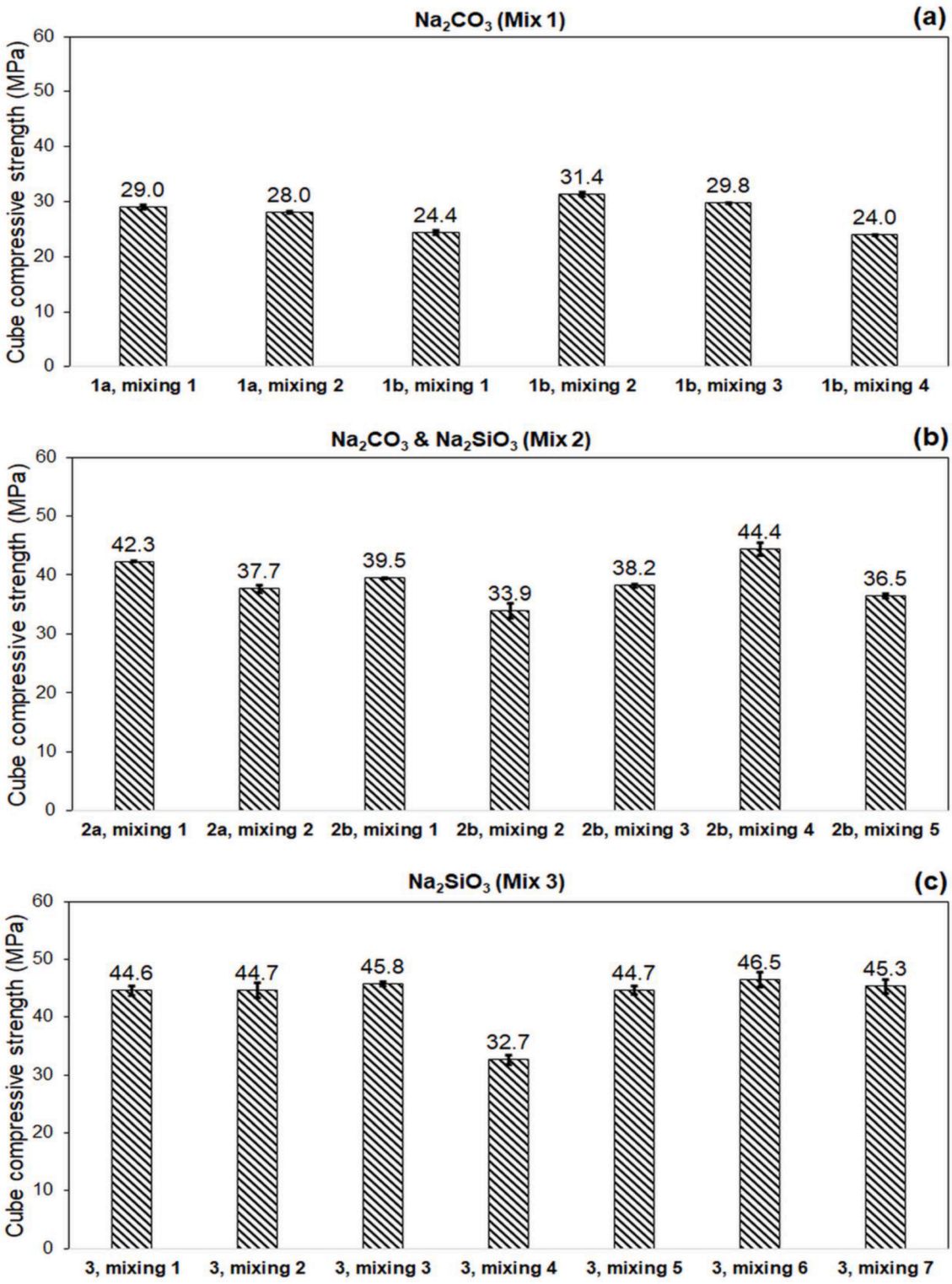

Fig. 2. Results of preliminary testing: effect of mixing procedure of 7-day strength.

deemed indicative of any trends; however a clear pattern that transpires is that trying to make a binder slurry with Na_2CO_3 and GGBS to then implement it to the aggregates in the mix, is the least good procedure, resulting in the lowest strengths and (based on observation) stiffer and less workable mixes (see mixing procedures 1b,mixing 1 and 1b,mixing 4). RILEM (2014) note the formation of hydrous sodium carbonate salts binding a large amount of water increasing the water demand of the mixes, which can have an impact if this formation happens during mixing. Otherwise, applying the Na_2CO_3 in solution ensuring the powder has thoroughly dissolved before implementing it into the mix appears to give a slight advantage in terms of strength, over mixing the Na_2CO_3 in powder form. It is possible that this is linked to the better control of Na_2CO_3 dissolution when supplied in solution rather than dry mixed. Namely, based on the authors' experience poorly dissolved Na_2CO_3 can lead to very low performance of resulting concrete. The authors observed that when prepared by unexperienced users (who were asked to replicate the authors' tests) and without meticulous mixing, the AAC mixes could give very poor results. For instance, mixes 1 and 2 were reported to be very dry and friable or not hardening properly even weeks later. The issue was investigated by the authors, and it transpired that poor mixing and especially poor dissolution of the Na_2CO_3 powder was at the root of such problems. When Na_2CO_3 was thoroughly dissolved, the mixes were appropriate in terms of fluidity, casting, setting and finish. Another possible explanation is that when Na_2CO_3 is used in powdered form it may have a slower release of alkali into the AAC as opposed to when it is provided in solution, leading to a slower rate of initial reaction hence lower strength gain (Yang et al., 2008). It should be noted however that the existing literature findings on the comparison of different one-part (i.e., alkaline activator supplied in powder form) versus two-part (alkaline activator supplied in solution) alkali-activated materials do not converge. For example, our findings that supplying the alkali in solution leads potentially to a higher strength are consistent with Nematollahi et al. (2015) making one-part geopolymer cement at ambient temperature, who reported that one-part fly ash geopolymer cement had a reduced strength by 13 MPa compared to an equivalent two-part geopolymer mix they tested; however Peng et al. (2014) using NaOH and Na_2CO_3 to activate low-quality kaolin calcined at temperatures between 650 and 1050ºC, found higher strengths for one-part geopolymers. On the other hand, Suwan and Fan (2017) found no differences in the reaction products of one and two-part fly-ash geopolymers when prepared with similar mixing ratios. (Note the different precursors used in these examples).

The mixing procedure with the highest strength was chosen (i.e., 1b, mixing 2) as the mix was overall good also in terms of fluidity/workability.

Consistently with mix 1, for mix 3 all mixing methods worked well giving small differences in the results except mixing 4 (where GGBS was implemented later, after the aggregates were wetted by part of the solution and water), and mixing 6, which was dry and unworkable (presumably due to the stickier, thicker solution) as opposed to all other batches that were fluid and workable, although it gave the highest 7-day strength (consistently with the procedure giving higher strength for mix 2, i.e. where the GGBS was mixed with the Na_2SiO_3). Mixing procedure 3 was thus adopted as it gave the next best strength for mix 3 (with very small difference compared to mixing procedure 6).

For mix 2, the results of the different procedures appear to be more variable pointing at a higher sensitivity to the mixing procedure. Consistently with mix 3 the worst strength in mix 2 was for mix 2b, mixing 3 where GGBS was implemented later, after the aggregates were wetted by part of the combined Na_2CO_3 and Na_2SiO_3 solution (mixed in all water). Mixing thoroughly the GGBS with the Na_2SiO_3 solution, then adding the Na_2CO_3 solution in the mix to implement the full binder mix on the aggregates gave the best results (2b, mixing 4), which is consistent with the method giving highest strengths for mix 3; this mixing procedure was thus adopted for mix 2. Conversely mixing the GGBS in a premixed, combined Na_2SiO_3 and Na_2CO_3 solution, gave the second lowest strength, 8 MPa lower than the best strength, which can be considered as a significant difference.

For all mixes, adding all water in the activator solution appears to work overall better despite the lower alkalinity, making the solution easier to mix uniformly with the dry ingredients (aggregates/GGBS).

Having chosen the three mixing procedures to use respectively for the three mixes, the main testing on the three mixes continued. Before casting the mixes into moulds, the slump of the mixes was measured immediately after mixing (BSI, 2009a). There was no true slump, as mixes 1 and mix 3 both collapsed with a height change of 220 mm, whereas mix 2 showed shear slump of 130 mm. Although overly liquid at the beginning, mix 3 started however setting very fast, so that unless the specimens were cast within the first 15–20 min, they were difficult to cast and vibration was becoming problematic, as specimens would not get a uniform consistency if cast too late. This is consistent with the literature reporting that initial setting times in alkali slag pastes activated with sodium silicate solution can begin as early as 15 min of reaction (Fernández-Jiménez and Puertas, 2003). Based on this, the casting of big batches for this mix was avoided to overcome problems linked to the fast initial setting, which can be attributed to the early calcium silicate hydrate (C–S–H) formation as silicate ions react with the Ca^{2+} ions from the slag (Fernández-Jiménez and Puertas, 2001). On the other hand, mixes 1 and 2 did not present the same problem as the alkali solution carbonate ions increase setting time (Fernández-Jiménez and Puertas, 2001 and 2003). Comparing the three mixes, mix 2 was reported to be the least good in terms of fluidity and finish (looking slightly drier and more porous) compared to mix 1 and 3. Generally, however, all three mixes would need 3–4 days before being ready for demoulding without getting damaged; this information is particularly important for curing method 1, because if placed in water too soon specimens are likely to start disintegrating.

3.2. Main experimental programme results

The following sections present results of the main experimental programme, which used the selected mixing sequences for each mix, based on the knowledge gained from the preliminary tests. All AAC concrete results are compared indicatively against those of CEM-I concrete of the same liquid to solid (water/cement) ratio and same cement/aggregate proportions as the AAC concrete mixes tested here (see Table 2) and cured according to method 1 (which is very common for regular cast-in-place concrete). The presented tests on CEM-I concrete were performed in a previous study and were published in Mengasini et al. (2021).

3.2.1. Cube compressive and splitting cylinder strengths

Average cube compressive strength results at 7, 28 and 56 curing times expressed to the nearest 0.5 MPa (BSI, 2019a) are shown in Fig. 3. Overall, all AAC mixes had high compressive strengths, fit for structural concrete. For mixes 2 and 3 strengths were comparable to CEM-I, at all curing ages, depending on the curing method. Mix 1 (Na_2CO_3 only) had much lower early compressive strengths compared to the respective strengths of mixes 2 and 3 with Na_2SiO_3. Based on solid-state NMR spectroscopy and X-Ray Diffraction study on sodium carbonate-sodium silicate activated slag mortars in Bernal et al. (2016) the earlier strength gain of mix 2 can be attributed to the reduced CO_3^{2-} concentration in the AAC system compared to mix 1 with Na_2CO_3-only activator. According to Bernal et al.'s (2016) explanation, for the latter system, which does not contain dissolved silicates, the Ca^{2+} released when slag dissolves interact with the CO_3^{2-} (from the activator) and are thus consumed in forming carbonate phases (calcium and mixed sodium-calcium carbonates) instead of developing C-S-H gels which are linked to high strengths. Conversely, due to their higher alkalinity, sodium silicate-containing AAC (i.e. mix 2 and 3) accelerate the slag dissolution compared to Na_2CO_3-only AAC systems, and the Si species from the sodium silicate component in the activator are used to form C-A-S-H within the first 24 h of reaction, which is the phase linked to strength increase. This therefore was concluded to be the cause of high early strength development of the Na_2SiO_3-containing AAC (Bernal et al., 2016). However, at later curing times Fig. 3 shows considerable strength gains for mix 1 (carbonate only). Based on the findings of detailed material characterisation by Bernal et al. (2015) this considerable strength increase is due to the formation of C-A-S-H type phases and hydrotalcite also in the Na_2CO_3-only AAC systems (as is mix 1), together with other (Ca,Al)-rich phases, except this starts after 7 days of curing versus after 1 day of curing in the mixed carbonate-silicate systems. This implies that after consumption of CO_3^{2-} from the alkaline activator (to form carbonate compounds), within a few days of reaction, Na_2CO_3-activated slag reaction mechanism proceeds similarly as in NaOH or Na_2SiO_3 AAC systems; this justifies the later increase in the mechanical strength in the Na_2CO_3-only AAC systems (Bernal et al., 2015). Consequently, the 7/28 day and 7/56 day strength ratios of mix 1 were the lowest of all mixes especially for curing methods 1 and 2 which showed a considerable strength gain during the whole period of curing (see Table 4). The strengths of mix 1 at 28 and 56 days of curing were lower than those of CEM-I and the other AAC mixes with Na_2SiO_3, however based on the 28-day strengths, mix 1 had adequate strengths for >40 MPa cube strength concrete (C30/40 concrete grade).

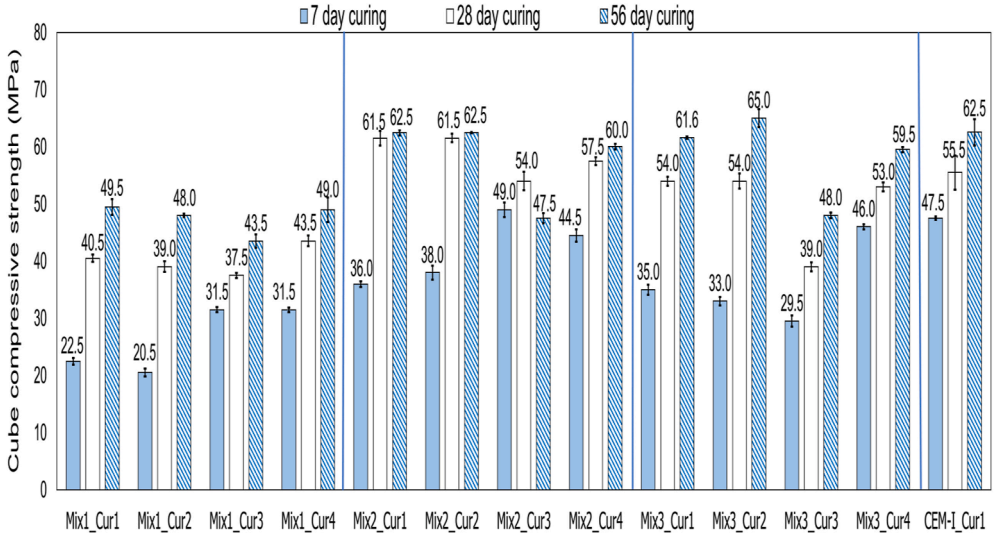

Fig. 3. Cube compressive strengths at different curing times.

Table 4
Evolution of cube compressive strength with curing time.

Mix #	7 day strength/28 day strength ratio	7 day strength/56 day strength ratio	28 day strength/56 day strength ratio
Mix1 Cur1	0.56	0.45	0.82
Mix1 Cur2	0.53	0.43	0.81
Mix1 Cur3	0.84	0.72	0.86
Mix1 Cur4	0.72	0.64	0.89
Mix2 Cur1	0.59	0.58	0.98
Mix2 Cur2	0.62	0.61	0.98
Mix2 Cur3	0.91	1.03	1.14
Mix2 Cur4	0.77	0.74	0.96
Mix3 Cur1	0.65	0.57	0.88
Mix3 Cur2	0.61	0.51	0.83
Mix3 Cur3	0.76	0.61	0.81
Mix3 Cur4	0.87	0.77	0.89
CEM-I_Cur1	0.86	0.76	0.89

It is interesting that for the mixes with Na_2CO_3 (mix 1 and mix 2), curing method 3 (thermal curing) and 4 (high humidity curing) gave the highest early strengths; this is consistent with observations on different AAC mixes without Na_2CO_3 activator (see e.g., Mavroulidou & Martynková, 2018 or Mavroulidou et al., 2021). However, with this curing, strength gain was very small at higher curing times and in fact, some apparent reversal in strength (decrease in strength) can be seen for mix 2 with curing method 3. This reversal in strength is difficult to explain and requires further investigation; it has been occasionally observed in other AAC systems tested at LSBU and could perhaps be attributed to thermal microcracks forming during thermal curing before placing the specimens in the water bath for further curing. Although the strength evolution of mix 1 was the most pronounced, all AAC mixes kept gaining strength in time, and depending on the curing method, mixes with Na_2SiO_3 eventually exceeded CEM-I mix strengths at 28 and/or 56 days of curing; this finding is in accord with round robin RILEM TC 247-DTA test across 15 laboratories worldwide, testing AAC systems (different to those presented here) as published in Provis et al. (2019); this showed increasing AAC strengths at 56 days of curing.

Fig. 4(a) represents the results of 28-day splitting cylinder tests and Fig. 4(b) correlates these to the cube compressive strength. Splitting tensile strength (f_t) results were found to be as expected for PC concrete, i.e., ca. 6–7% of the compressive strength, with a very strong correlation with the compressive strength despite some expected scatter.

3.2.2. *Water absorption and effective porosity*

Fig. 5 (a)-(b) represent respectively the average water absorption by a 30 min immersion and capillary action for 4 h. Fig. 5(c) represents the effective porosity of the hardened concrete samples based on helium porosimetry (error bars in Fig. 3 (a)–(c) show maximum and minimum values). The results are variable, but generally AAC mix absorption has clearly increased compared to CEM-I mix, although values remain below 10% which is acceptable (Neville, 1995). The results also indicate that (a) the Na_2SiO_3 mix (mix 3) has generally a lower absorption than the other AAC mixes; (b) curing method 3 (thermal curing) generally results in the lowest absorption, whereas for the other curing methods the differences are not pronounced; the lowest water absorption of curing method 3 is consistent with Bakharev et al. (1999) as well as results of the LSBU group on other AAC systems (Mavroulidou & Martynková, 2018 and Mavroulidou and Shah, 2021), and according to Bakharev et al. (1999) it could be due to reduced drying shrinkage upon thermal curing; (c) there appears to be some evolution of the porosity in time which suggests that reaction product formation evolves in time. The visible increase in the capillary absorption of the Na_2CO_3 only mix (mix 1) could be linked to a pore

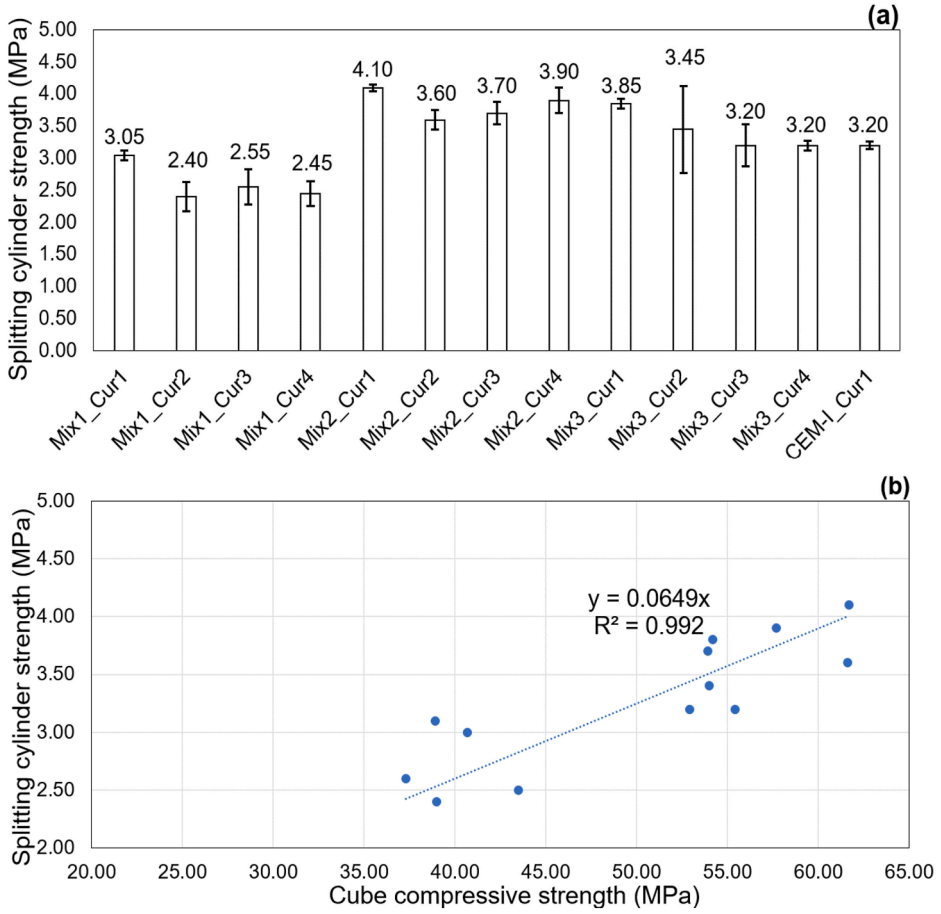

Fig. 4. (a) Splitting cylinder strength results; (b) splitting cylinder and cube compressive strength correlation (28 day-cured concrete mixes).

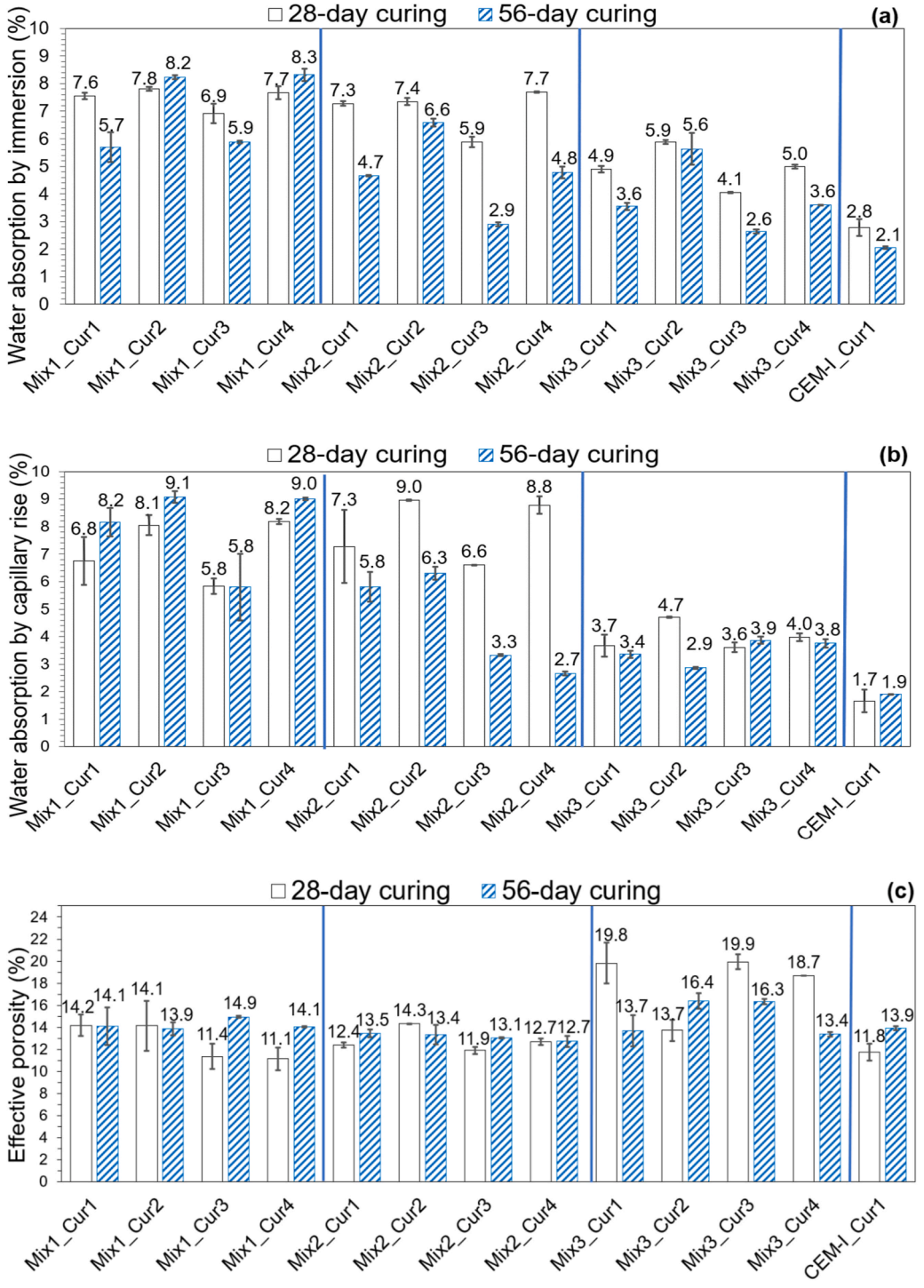

Fig. 5. Water absorption and effective porosity at different curing times (a) absorption by immersion; (b) absorption by capillary action; (c) effective porosity.

refinement (finer interconnecting pores encouraging higher capillary rise) resulting from the development of reaction products in the pores, as testified in Bernal et al. (2015). The porosity results do not show overall a clearly higher effective porosity for AAC than CEM-I mix porosity (reflecting the higher AAC absorption), except for mix 3 (Na_2SiO_3-only). Surprisingly, this is the AAC mix with the overall lowest water absorption of all AAC mixes; it is however noteworthy that in other Na_2SiO_3 only mixes tested at LSBU containing higher Na_2SiO_3 content and/or having higher liquid to solid ratio, individual measurements of porosities did not exceed 15% or at most 17% depending on the mix design (see e.g., Pagadala, 2018 or Mengasini et al., 2021). It can however be noted that although a higher porosity and water absorption are normally linked with a reduced PC concrete durability, as deleterious ions

would be more easily transported, the corrosion and sulphate resistance results presented in the following sections do not show a clear decline in the AAC mix durability compared to CEM-I mix, which according to Shi et al. (2006) could be attributed to the fine pore-size distribution of AAC.

3.2.3. Corrosion resistance

Table 5 shows the corrosion rates and the rebar mass loss due to corrosion; indicatively the corrosion rate of CEM-I based on Mengasini et al. (2021) is also shown. Based on these, AAC mixes clearly had a higher resistance to corrosion compared to PC concretes. CEM-I mix corrosion rate was 4.2–5.6 times higher compared to AAC mixes, its mass loss was 7.5–10 times higher and one rebar in one of the CEM-I specimens had disintegrated completely. Of the AAC mixes, mix 1 (Na_2CO_3 only) had the highest corrosion rate and mass loss whereas mix 3 (Na_2SiO_3 only) had the lowest corrosion rate and mass loss, but overall, the differences between the AAC mixes were not considerable. Also, cracks were observed on the surfaces of CEM-I samples due to the internal pressures exerted as rebar rusts (see Fig. 6(c)). The good state of the embedded rebars in the AAC concrete mixes at the end of the corrosion testing is testified by Fig. 6(a) and (b) showing respectively the rebars before and after extraction from the concrete. Conversely the clear damage to the CEM-I concrete specimen and the embedded rebar is visible respectively in Fig. 6(c) and (d). The AAC concrete mixes thus

Table 5
Accelerated corrosion test results: corrosion rate and (%) average mass loss.

Mix #	Corrosion rate (mm/year)	Average mass loss (%)
Mix 1	2.98	1.2
Mix 2	2.56	1.1
Mix 3	2.22	0.9
CEM-I (Mengasini et al., 2021)	12.45	>9% [a]

[a] In Mengasini et al. (2021) measurements could not be taken in one of the CEM-I specimen rebars as it had disintegrated.

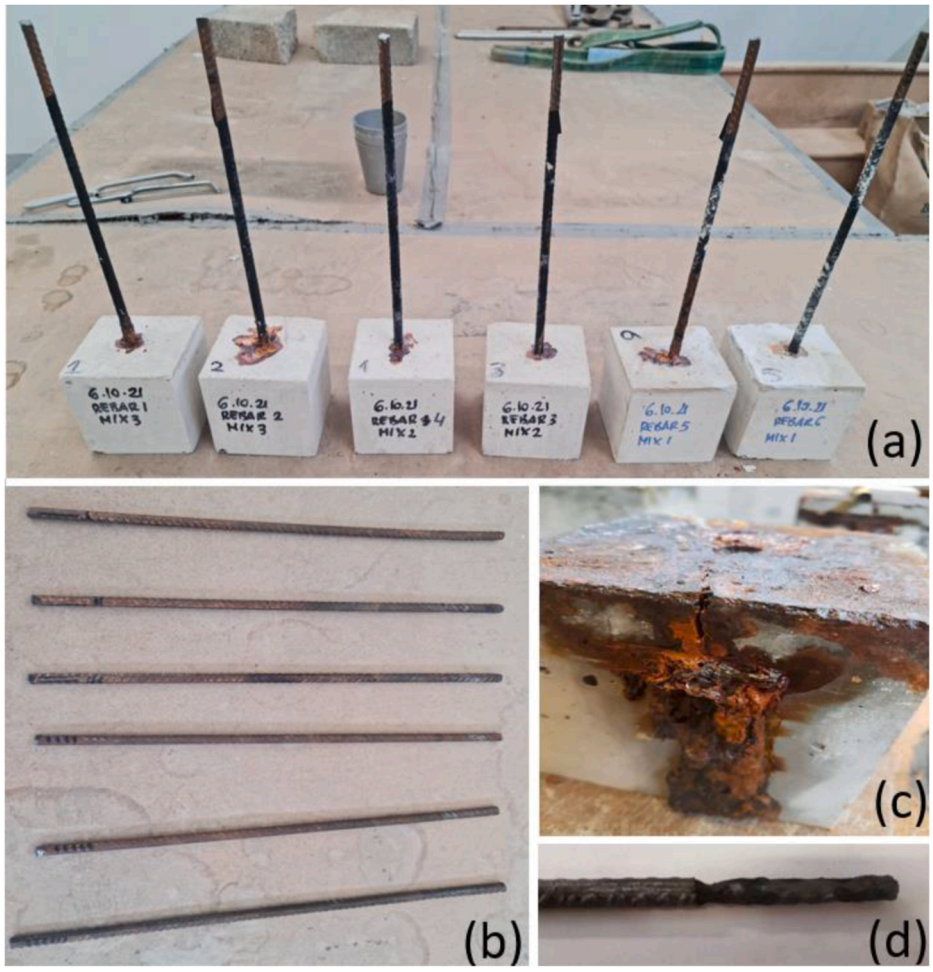

Fig. 6. Effect of chlorides on embedded steel rebars: (a)–(b) AAC mixes; (c)–(d) CEM-I mix.

had a better corrosion resistance although their effective porosity and absorption were higher than those of CEM-I concrete (see Fig. 5(c)). This is unlike regular PC for which low porosities are required to minimise fluid ingress as a way of increasing durability. On the other hand, as argued in Mengasini et al. (2021), in AAC the durability is likely due to post-pozzolanic reactions in the cement pores over time and the formation of extremely stable C-A-S-H binder. C-A-S-H phases were indeed detected in Na_2CO_3 and Na_2CO_3-Na_2SiO_3 activated GGBS AAC systems by Bernal et al. (2015) and (2016) respectively. RILEM (2014), also points out that in AAC, gel chemistry can help in maintaining durability despite higher porosity. Moreover, for AAC systems with Na_2CO_3 Bernal et al. (2015) noted a very high tortuosity in the pore network, which is again favourable as it delays transport. A thirty to forty times slower chloride ingress than in PC was also observed in GGBS AAC by Krivenko et al. (2016), while Gluth et al. (2020) reported GGBS concretes to have the highest resistance to chloride attack of all AAC tested in the round robin RILEM TC 247-DTA experiments. As summarised in Mengasini et al. (2021), a number of researchers attributed the reduced chloride ingress to the microstructure (fine pore structure) of the AAC slag concretes and/or their ability to bind Cl^- into hydrotalcite-like hydration products; (see e.g. discussions in van Deventer et al., 2010; Ma et al., 2016; Khan et al., 2016; Ke et al., 2017 (a), (b)).

3.2.4. Sulphate attack resistance

The length change at different times of specimens immersed in Na_2SO_4 solution is shown in Fig. 7(a)–(c). Most measurements on AAC (with two exceptions for mix 2 and one exception for mix 3) did not show any expansion when exposed to sulphate; even in the three instances where some expansion was noted this was much lower than that of CEM-I, which showed some initial shrinkage but then expanded considerably. Mengasini et al. (2021) observed that CEM-I samples had cracked considerably along the edges; together with the measured expansion this corroborates the assumption of ettringite formation. Conversely the tested AAC cubes here had no visible cracks. This is again in agreement with RILEM TC 247-DTA round robin tests published in Provis and Winnefeld (2018), showing no considerable expansion/damage to any of the AAC tested, as well as with results in Mengasini et al. (2021) studying AAC systems cured and /or mixed with seawater and then exposed to sulphate attack. The cube compressive strength measured after 90 days of exposure (see Fig. 8) showed that mix 1 strength appeared to be unaffected by the exposure to sulphate, as for all methods the strengths recorded were same or slightly higher than those recorded at 56-day cube compressive strength testing. Mix 3 showed variable results depending on the curing method, however on the main it maintained the strengths of the 56-day cube testing, considering the variability of concrete batches; similarly, for CEM-I mix there is an indication of a 3.5 MPa reduction in strength after exposure to sulphate but it may not be significant considering the usual variation in the strength of concrete batches. Conversely mix 2 showed a marked decrease in strength after exposure to sulphates. This is difficult to explain and requires further investigation, as it is an intermediate mix between mixes 1 and 3 which did not present similar problems and although mix 2 was reported to look more porous and drier than mix 1 and 3 during casting (which could have justified a higher ingress of sulphates) the porosity testing results after curing did not corroborate this observation.

4. Conclusions

This paper studied the performance of GGBS AAC concrete under different mixing and curing regimes using Na_2CO_3 activator and activator mixes of Na_2CO_3 plus Na_2SiO_3, compared to Na_2SiO_3 used as the sole activator. The rationale of the research was the potential further improvement in the sustainability of AAC if using Na_2CO_3 in the alkaline activator system, because Na_2CO_3 is cheaper and it is less environmentally damaging to obtain it, compared to the production of Na_2SiO_3 or NaOH (most common activators in AAC systems).

The main findings were that:

- most mixing sequences worked well giving comparable strengths but lower strengths were obtained when mixing GGBS directly in Na_2CO_3 before implementing Na_2CO_3 to the aggregates or wetting the dry aggregates with part of the liquid components of the mix (including activator solutions) then implementing the GGBS;
- mixing the Na_2SiO_3 with the GGBS (and in combined activator systems, implementing Na_2CO_3 after Na_2SiO_3 addition to the GGBS) and mixing the binder systems thus obtained with the aggregates would work well;
- mixing the whole water required for the concrete mix with the activator solutions appeared to work best;
- there was also some indication that providing Na_2CO_3 in solution could give better strengths than if mixed in powder form;
- curing at ambient temperature and a higher exposure to moisture at all curing times were better in sustaining AAC mix strength gain in time whereas thermal curing gave the highest early strengths and generally the lowest absorption and porosities but led to limited strength increase in time.
- Overall, compressive strengths of all AAC mixes were suitable for structural concrete, although strengths of AAC systems including Na_2SiO_3 had the highest strengths at all curing conditions and ages. For the mix with Na_2CO_3 only (suitable for C30/40 grade concrete vs C50/60 concrete for the mixes containing Na_2SiO_3) strengths kept evolving more considerably with curing time despite the lower early strengths.
- Indirect tensile strength had a similar relationship to the compressive strength as for PC concrete.
- All mixes with AAC performed better in terms of chloride attack (accelerated corrosion test) despite their higher water absorption and in most cases porosity, compared to the Portland Cement mix. They had however a variable performance in the sulphate attack test, with AAC with Na_2CO_3 as the sole activator being the least affected in terms of strength after exposure to sulphates.

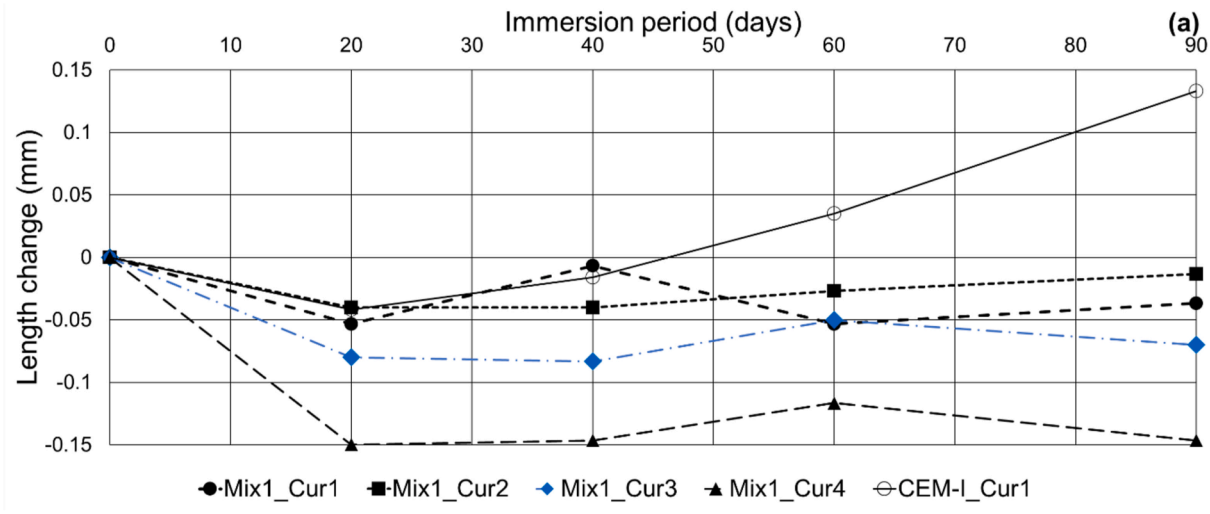

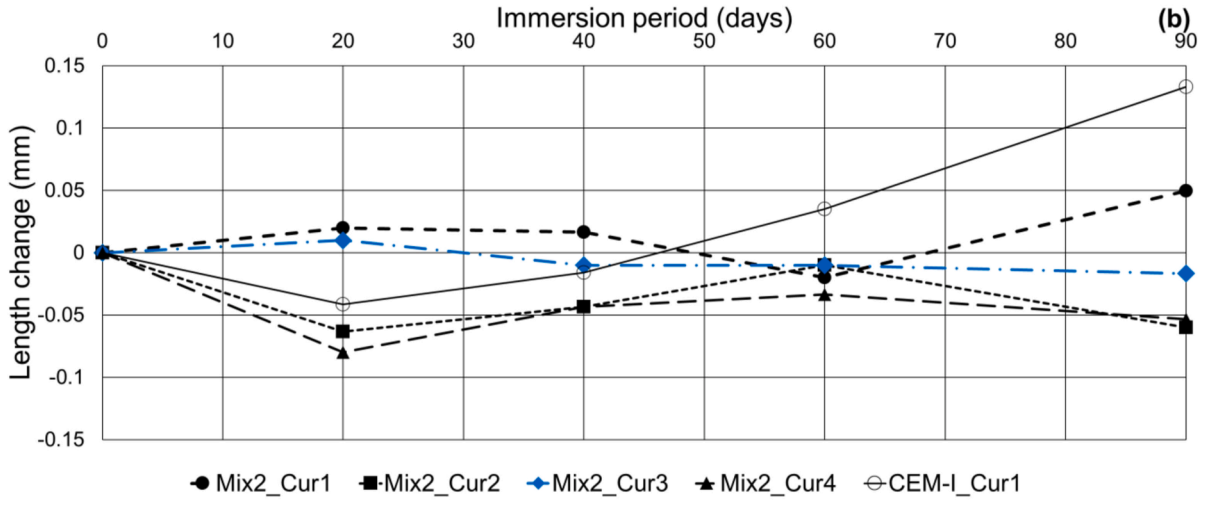

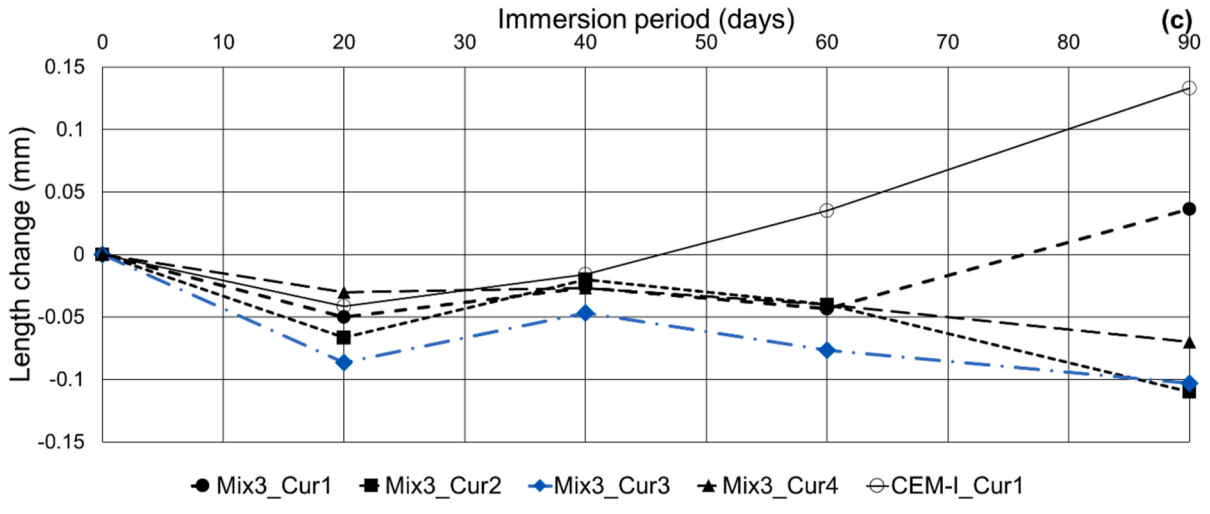

Fig. 7. Specimen length change during immersion in sulphate: (a) Mix 1; (b) Mix 2; (c) Mix 3.

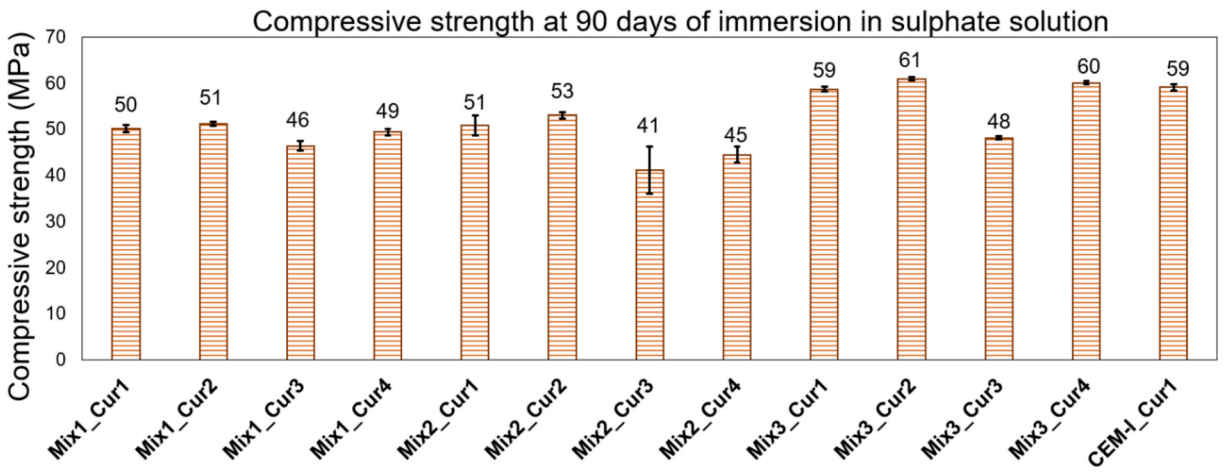

Fig. 8. Specimen compressive strength after 90 days immersion in Na_2SO_4 solution.

Overall, from the above, it can be concluded that unless early strength gain is required, Na_2CO_3-activated GGBS AAC can give concrete the required properties for structural applications, if properly mixed and cured, while being cheaper and of a lower environmental footprint than other common AAC systems. Combining Na_2CO_3 with Na_2SiO_3 would also have a reduced cost and environmental impact compared to using AAC with Na_2SiO_3 as sole activator, with similar strengths as the latter AAC even at earlier ages; however, the sulphate exposure results showed a reduction in strength when combining Na_2CO_3 with Na_2SiO_3 which needs further investigation.

5. CRediT authorship contribution statement

Mavroulidou: Conceptualization; Methodology; Supervision; Funding acquisition; Formal analysis; Visualisation; Writing - original draft (lead), Writing - review & editing. **Sanam:** Investigation**;** Formal analysis; Writing - review & editing. **Mengasini**: Investigation**;** Formal analysis; Writing - review & editing.

Declaration of competing interest

The authors declare that they have no known competing financial interests or personal relationships that could have appeared to influence the work reported in this paper.

Data availability

Data will be made available on request.

Acknowledgement

The research was performed at London South Bank University (LSBU) using LSBU resources. It received supporting funding from the CCiBSE Research Centre (LSBU). The authors are grateful to Graham Bird, Paul Elsdon and Christopher Gray for assisting with the experiments.

References

Abdalqader, A.F., Jin, F., Al-Tabbaa, A., 2016. Development of greener alkali-activated cement: utilisation of sodium carbonate for activating slag and fly ash mixtures. J. Clean. Prod. 113, 66–75.

American Society of Testing and Materials (Astm), 2000. Standard Practice for Preparing, Cleaning, and Evaluating Corrosion Test Specimens, ASTM G1-90, G01 Committee ASTM International, American Society for Testing and Materials, Designation G15-99b (Revised) 03.02.2000. ASTM, West Conshohocken.

Bakharev, T., Sanjayan, J.G., Cheng, Y.-B., 1999. Effect of elevated temperature curing on properties of alkali-activated slag concrete. Cement Concr. Res. 29, 1619–1625.

Bernal, S., Provis, J.L., Myers, R.J., San Nicolas, R., van Deventer, J.S.J., 2015. Role of carbonates in the chemical evolution of sodium carbonate-activated slag binders. Mater. Struct. 48, 517–529.

Bernal, S.A., San Nicolas, R., van Deventer, JSJ, Provis, J.L., 2016. Alkali-activated slag cements produced with a blended sodium carbonate/sodium silicate activator. Adv. Cement Res. 28 (4), 262–273.

British Standards Institution (BSI), 2009a. BS EN 12350-2:2009: Testing Fresh Concrete, Part 2: Slump Test. BSI, London.

British Standards Institution, 2011. BS EN 1881-122:2011: Testing Concrete Part 122: Method for Determination of Water Absorption. BSI, London.

British Standards Institution (BSI), 2019a. BS EN 12390-3:2019: Testing Hardened Concrete. Part 3: Compressive Strength of Test Specimens. BSI, London.

British Standards Institution (BSI), 2019b. BS EN 12390-6:2019: Testing Hardened Concrete -Part 6: Tensile Splitting Strength of Test Specimens. BSI, London.

Criado, M., Provis, J.L., 2018. Alkali activated slag mortars provide high resistance to chloride-induced corrosion of steel. Front. Mater. 5, 34. https://doi.org/10.3389/fmats.2018.00034.

Davidovits, J., 2013. Geopolymer Cement. A Review 2013. Geopolymer Institute. [Online]. Available from: http://www.geopolymer.org/library/technical-papers/21-geopolymer-cement-review-2013. 11/08/13.

Ellis, L.D., Badel, A.F., Chiang, M.L., Park, R.J-Y, Chiang, Y-M, 2020. Toward electrochemical synthesis of cement-An electrolyzer-based process for decarbonating

$CaCO_3$ while producing useful gas stream. Proc. Natl. Acad. Sci. USA 117 (23), 12584–12591.
Fernández-Jiménez, A., Puertas, F., 2001. Setting of alkali-activated slag cement. Influence of activator nature. Adv. Cement Res. 13 (3), 115–121.
Fernández-Jiménez, A., Puertas, F., 2003. Effect of activator mix on the hydration and strength behaviour of alkali-activated slag cements. Adv. Cement Res. 15 (3), 129–136.
Garcia-Lodeiro, I., Fernández-Jimenez, A., Palomo, A., 2015. Cements with a low clinker content: versatile use of raw materials. J. Sustain. Cement-Based Mater. 4 (2), 140–151.
Gluth, G.J.G., Arbi, K., Bernal, S.A., et al., 2020. RILEM TC 247-DTA round robin test: carbonation and chloride penetration testing of alkali-activated concretes. Mater. Struct. 2020 (53), 21. https://doi.org/10.1617/s11527-020-1449-3.
Imbabi, M., Carrigan, C., McKenna, S., 2012. Trends and developments in green cement and concrete technology. Int. J. Sustain. Built Environ. 1 (2), 194–216.
Jamieson, E., McLellan, B., van Riessen, A., Nikraz, H., 2015. Comparison of embodied energies of ordinary Portland cement with bayer-derived geopolymer products. J. Clean. Prod. 99, 112–118.
Ke, X., Bernal, S.A., Hussein, O.H., Provis, J.L., 2017a. Chloride binding and mobility in sodium carbonate-activated slag pastes and mortars. Mater. Struct. 50, 252. https://doi.org/10.1617/s11527-017-1121-8.
Ke, X., Bernal, S.A., Provis, J.L., 2017b. Uptake of chloride and carbonate by Mg-Al and Ca-Al layered double hydroxides in simulated pore solutions of alkali-activated slag cement. Cement Concr. Res. 100, 1–13. https://doi.org/10.1016/j.cemconres.2017.05.015.
Khan, M., Kayali, O., Troitzsch, U., 2016. Chloride binding capacity of hydrotalcite and the competition with carbonates in ground granulated blast furnace slag concrete. Mater. Struct. 49 (11), 4609–4619.
Kim, T., Kang, C., 2020. The mechanical properties of alkali-activated slag-silica fume cement pastes by mixing method. Int. J. Concrete Struct. Mater. 14, 41.
Kovtun, M., Kearsley, E.P., Shekhovtsova, J., 2015. Chemical acceleration of a neutral granulated blast-furnace slag activated by sodium carbonate. Cement Concr. Res. 72, 1–9.
Krivenko, P., 2017. Why alkaline activation - 60 Years of the theory and practice of alkali-activated materials. J. Ceram. Sci. Technol. 8 (3), 323–334. https://doi.org/10.4416/JCST2017-00042.
Krivenko, P., Rudenko, I., Konstantynovskyi, O., Boiko, O., 2021. Restriction of Cl^- and SO_4^{2-} ions transport in alkali activated slag cement concrete in seawater. IOP Conf. Ser. Mater. Sci. Eng. 1164, 012066.
Krivenko, P., Cao, H., Weng, L., Petropavlovskii, O., 2016. High-performance alkali-activated cement concretes for marine engineering applications. In: Yilmaz, S., Ozmen, H. (Eds.), High Performance Concrete Technology and Applications. Intech. Chapter 8.
Li, Y., Sun, Y., 2000. Preliminary study on combined-alkali-slag paste materials. Cement Concr. Res. 30, 963–966.
Luukkonen, T., Abdollahnejad, Z., Yliniemi, J., Kinnunen, P., Illikainen, M., 2018. One-part alkali-activated materials. Rev. Cement Concrete Res. 103, 21–34.
Ma, Q., Nanukuttan, S.V., Basheer, P.A.M., Bai, Y., Yang, C., 2016. Chloride transport and the resulting corrosion of steel bars in alkali activated slag concretes. Mater. Struct. 49, 3663–3677. https://doi.org/10.1617/s11527-015-0747-7.
Mavroulidou, M., 2017. Mechanical properties and durability of concrete with water cooled copper slag aggregate. Waste and Biomass Valorisation 8, 1841–1854.
Mavroulidou, M., Martynková, R., 2018. A study of alkali-activated concrete mixes with ground granulated blast furnace slag. J. Global Netw. Environ. Sci. Technol. 20, 216–225.
Mavroulidou, M., Gray, C., Gunn, M.J., Pantoja-Muñoz, L., 2021. A study of innovative alkali-activated binders for soil stabilisation in the context of engineering sustainability and circular economy. Circ. Econ. Sustain. https://doi.org/10.1007/s43615-021-00112-2.
Mavroulidou, M., Shah, S., 2021. Alkali-activated slag concrete with paper industry waste. Waste Manag. Res. https://doi.org/10.1177/0734242X20983890.
Mengasini, L., Mavroulidou, M., Gunn, M.J., 2021. Alkali-activated concrete mixes with ground granulated blast furnace slag and paper sludge ash in seawater environments. Sustain. Chem. Pharm. 20, 100380.
Nematollahi, B., Sanjayan, J., Shaikh, F.U.A., 2015. Synthesis of Heat and Ambient Cured One-Part Geopolymer Mixes with Different Grades of Sodium Silicate.
Neville, A.M., 1995. Properties of Concrete, fourth ed. Longman, Harlow.
Nodehi, M., Ozbakkaloglu, T., Gholampour, A., Mohammed, T., Shi, X., 2022. The effect of curing regimes on physico-mechanical, microstructural and durability properties of alkali-activated materials: a review. Construct. Build. Mater. 321, 126335.
Pagadala, M.K., 2018. Experimental Investigation on Alkali-Activated Concrete. MSc Dissertation (unpublished). London South Bank University.
Palacios, M., Puertas, F., 2011. Effectiveness of mixing time on hardened properties of waterglass-activated slag pastes and mortars. ACI Mater. J. 108, 73–78.
Palomo, A., Krivenko, P., Garcia-Lodeiro, I., Kavalerova, E., Maltseva, O., Fernández-Jiménez, A., 2014. A review on alkaline activation: new analytical perspectives. Mater. Construcción 64 (315), e022. https://doi.org/10.3989/mc.2014.00314.
Parathi, S., Nagarajan, P., Shasikala, A.P., 2021. Ecofriendly geopolymer concrete: a comprehensive review. Clean Technol. Environ. Policy 23, 1701–1713. https://doi.org/10.1007/s10098-021-02085-0.
Passuello, A., Rodríguez, E.D., Hirt, E., Longhi, M., Bernal, S.A., Provis, J.L., Kirchheim, A.P., 2017. Evaluation of the potential improvement in the environmental, footprint of geopolymers using waste-derived activators. J. Clean. Prod. 166, 680–689.
Provis, J.L., Arbi, K., Bernal, S.A., et al., 2019. RILEM TC 247-DTA round robin test: mix design and reproducibility of compressive strength of alkali-activated concretes. Mater. Struct. 52, 99. https://doi.org/10.1617/s11527-019-1396-z.
Provis, J.L., Winnefeld, F., 2018. Outcomes of the round robin tests of RILEM TC 247-DTA on the durability of alkali-activated concrete. In: MATEC Web of Conferences. International Conference on Concrete Repair, Rehabilitation and Retrofitting (ICCRRR 2018), 19-21 Nov 2018. EDP Sciences, Cape Town, South Africa. https://doi.org/10.1051/matecconf/201819902024.
RILEM, 2014. In: Provis, J., van Deventer, J. (Eds.), Alkali Activated Materials. State-Of-The-Art Report, RILEM TC 224-AAM. Springer/RILEM Dordrecht.
Shi, C., Krivenko, P.V., Roy, D., 2006. Alkali-Activated Cements and Concretes. Taylor & Francis, New York.
Salas, D.A., Ramirez, A.D., Ulloa, N., Baykara, H., Boero, A.J., 2018. Life cycle assessment of geopolymer concrete. Concrete Build. Mater. 190, 170–177.
Suwan, T., Fan, M., 2017. Effect of manufacturing process on the mechanisms and mechanical properties of fly ash-based geopolymer in ambient curing temperature. Mater. Manuf. Process. 32 (5), 461–467. https://doi.org/10.1080/10426914.2016.1198013.
Tchakouté, H.K., Rüscher, C.H., Kong, S., Kamseu, E., Leonelli, C., 2016. Geopolymer binders from metakaolin using sodium waterglass from waste glass and rice husk ash as alternative activators: a comparative study. Construct. Build. Mater. 114, 276–289.
van Deventer, J.S.J., Provis, J.L., Duxson, P., et al., 2010. Chemical research and climate change as drivers in the commercial adoption of alkali activated materials. Waste Biomass Valorisation 1, 145–155.
Xu, H., Provis, J.L., Van Deventer, J.S.J., Krivenko, P.V., 2008. Characterization of aged slag concretes. ACI Mater. J. 102, 131–139.
Yang, K.H., Song, J.K., Song, K.I., 2013. Assessment of CO_2 reduction of alkali-activated concrete. J. Clean. Prod. 39, 265–272.
Yang, K.H., Song, J.K., Ashour, A.F., Lee, E.T., 2008. Properties of cementless mortars activated by sodium silicate. Construct. Build. Mater. 22, 1981–1989.